

Instruction-Based Molecular Graph Generation with Unified Text-Graph Diffusion Model

Yuran Xiang¹

Haiteng Zhao¹

Chang Ma²

Zhi-Hong Deng¹

¹Peking University ²The University of Hong Kong
xiangyuranyp@stu.pku.edu.cn {zhaohaiteng,zhdeng}@pku.edu.cn changma@connect.hku.hk

Abstract

Recent advancements in computational chemistry have increasingly focused on synthesizing molecules based on textual instructions. Integrating graph generation with these instructions is complex, leading most current methods to use molecular sequences with pre-trained large language models. In response to this challenge, we propose a novel framework, named **UTGDiff (Unified Text-Graph Diffusion Model)**, which utilizes language models for discrete graph diffusion to generate molecular graphs from instructions. UTGDiff features a unified text-graph transformer as the denoising network, derived from pre-trained language models and minimally modified to process graph data through attention bias. Our experimental results demonstrate that UTGDiff consistently outperforms sequence-based baselines in tasks involving instruction-based molecule generation and editing, achieving superior performance with fewer parameters given an equivalent level of pretraining corpus. Our code is available at <https://github.com/ran1812/UTGDiff>.

Introduction

Molecules, as fundamental units of matter, possess structures and properties that determine the characteristics of substances. Research into novel molecules is pivotal for chemistry, biology, and drug discovery (Schneider and Fechner 2005; Hughes et al. 2011), as these fields depend on the discovery of molecules with specific properties. A significant challenge in drug discovery is designing molecules that exhibit desired features, maintain structural stability, and interact with specific targets (Hartenfeller and Schneider 2011). Traditionally, this process has been resource-intensive and time-consuming (Dickson and Gagnon 2009; Khanna 2012). However, recent advancements in deep learning have revolutionized drug design by offering cost-effective methods (Nag et al. 2022; Askar et al. 2023), drawing significant attention to the research of generating drug-like molecules (Bagal et al. 2021; Schneuing et al. 2022).

In this work, we aim to bridge the gap between molecular structures and natural language, designing a generative model that functions akin to a drug design expert (illustrated in Figure 1). By receiving specific instructions, this model can precisely generate candidate molecules with the indicated characteristics. We focus on tasks including *instruction-based molecule generation* (Edwards et al. 2022)

and *molecule editing* (Fang et al. 2023), striving to integrate two modalities of information in drug design: aligning text descriptions to ensure desired properties and generating graph structures that represent potential molecules.

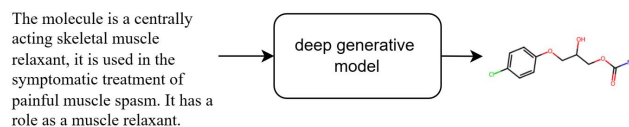


Figure 1: A deep generative model that works like a drug design specialist, with instruction input and molecule output.

One widely adopted approach involves generating molecular strings from instructions, such as SMILES or SELFIES (Weininger 1988; Krenn et al. 2020), which serve as a stop-gap for describing molecular graphs using language. Several recent studies have explored this method by employing auto-regressive language models (Edwards et al. 2022; Liu et al. 2023d; Pei et al. 2023), deploying large language models (Achiam et al. 2023; Ye et al. 2023; AI4Science and Quantum 2023), or modifying existing molecules based on specified instructions (Liang et al. 2023).

However, despite these advancements, current methods face significant challenges. The primary limitation of molecular strings lies in their insufficient capability to accurately represent complex molecular structures, as it is widely recognized that they lack spatial structure information such as neighborhood (Jiang et al. 2022; Wu et al. 2023; Song et al. 2020), which could limit performance. Additionally, aligning the language space with the molecular space often results in deviations from natural molecular distributions, such as generating unstable or rare structures through simple string reassembly (Druchok et al. 2021). It is therefore essential to develop a multimodal model that possesses robust molecular structure representational capabilities while maintaining instruction-following abilities.

As a non-sequential data structure, graph generation capacity could be constrained by fixed orders imposed by auto-regressive models. This limitation motivates our usage of diffusion, a powerful non-sequential generative model. Therefore, we propose the *Unified Text-Graph Diffusion Model (UTGDiff)*, a novel diffusion framework for text-guided graph generation. UTGDiff extends vanilla trans-

former as graph denoising networks through attention bias from graph edge categories, ensuring a strong capacity for learning graph structure representations and executing instruction texts without additional graph encoding modules. The equivariance of our model in graph structure ensures structural modeling abilities beyond asymmetric SMILES (O’Boyle and Dalke 2018; Arús-Pous et al. 2019).

We performed extensive experiments on the pre-trained UTGDiff model across diverse tasks. Our results show that UTGDiff achieves improved outcomes over language model baselines in drug design tasks (instruction-based molecule generation and molecule editing) despite its small parameter size (125M). Additionally, our use of a diffusion-generation pipeline and text-graph denoising network achieves a relatively high accuracy of over 85% in terms of chemical validity. In summary, our contributions are:

- We present a unified text-graph diffusion framework for instruction-based graph generation, enabling the creation of molecular structures that are instructed by text and represent accurate chemical structures.
- We propose UTGDiff, which advances the state of the art by employing this unified text-graph transformer that effectively captures the features of both graph and text data. The model distinguishes itself from prior work by enhancing molecular representation and generation.
- Experimental results demonstrate that UTGDiff outperforms existing language model baselines in several critical areas of drug design, including instruction-based molecule generation and molecule editing, with an equivalent level of pretraining corpus.

Related Works

Molecule Generation Early attempts at molecule generation introduced sequence-based models for SMILES strings (Dai et al. 2018; Gómez-Bombarelli et al. 2018). Due to the lack of structural information, recent studies have explored graph-based methods, including auto-regressive models (Grisoni et al. 2020; You et al. 2018), VAEs (Simonovsky and Komodakis 2018; Jin, Barzilay, and Jaakkola 2018; Liu et al. 2018), GANs (De Cao and Kipf 2018), and Normalizing Flows (Ma and Zhang 2021; Zang and Wang 2020). A relatively novel approach, offering superior performance and better scalability on larger molecules, is Graph Diffusion (Niu et al. 2020; Jo, Lee, and Hwang 2022; Vignac et al. 2022), which serves as our foundational framework.

Conditional Molecule Generation Conditional molecule generation, an important topic in molecule generation, aims to generate a molecular graph that satisfies a specific property. Early attempts are based on a scalar property such as dipole moment μ and p-logP scores (the octanol-water partition coefficients) (Li, Zhang, and Liu 2018; Huang et al. 2023). More complex conditions involve textual instructions, with existing solutions including sequence-based generation (Edwards et al. 2022; Christofidellis et al. 2023; Liu et al. 2023d; Li et al. 2023; Pei et al. 2024) and multimodal generation employing a text encoder and graph generative network (Su et al. 2022; Liu et al. 2024).

Cross-Modal Molecule Models In addition to the instruction-based cross-modal molecule generation models discussed above, some studies represent molecules and text in cross-modal models for molecule property prediction or text generation tasks (Liu et al. 2023c; Zhao et al. 2024; Liu et al. 2023a), employing contrastive alignment, cross-modal projector, or unified text-graph backbone.

Discrete Diffusion Previous Gaussian noise in continuous diffusion models has been shown to be insufficient for discrete data structure. As a solution, researchers introduced the discrete diffusion method, initially discussed in text diffusion (Austin et al. 2021; He et al. 2022) and later adapted for graph data (Vignac et al. 2022; Kong et al. 2023).

Preliminaries

The objective of the instruction-based molecule generation task is to generate a molecular graph $G = (V, E)$ from a given textual description S specifying molecular functions and properties. The graph consists of m nodes $V \in \mathbb{R}^{m \times a}$, which represent node attributes, and edges $E \in \mathbb{R}^{m \times m \times b}$, which represent edge attributes. Each attribute $v_i \in \mathbb{R}^a$ and $e_{i,j} \in \mathbb{R}^b$ is a one-hot vector representing the categories of nodes and edges, respectively. The instruction text is defined as $S = [s_1, \dots, s_n]$, where s_i denotes the i -th token, and n is the length of the instruction. The goal is to perform conditional graph generation $V, E \sim P(V, E | S)$.

Method

Overview of Diffusion Framework

We propose a text-conditioned diffusion framework for molecular graph generation, as depicted in Figure 2. As a generative model, the diffusion model iteratively refines random noise into structured data through a series of transformations. It involves the forward process, which gradually adds noise to data via a noise model, and the reverse process, which denoises the data to recover the original structure using a denoising network. At each reverse step, the model estimates and removes the noise component, progressively generating the final structure. The core component of our framework is the novel unified text-graph denoising network, described in the Reverse Process section.

Forward Process and Noise Model

The forward process, associated with the noise model q , progressively adds noise to corrupt the clean graph G^0 , creating an increasingly noisy graph sequence (G^1, \dots, G^T) :

$$q(G^{1:T} | G^0) = \prod_{t=1}^T q(G^t | G^{t-1}) \quad (1)$$

Since traditional Gaussian noise is not suitable for graphs due to its disruption of sparsity and graph theory properties such as connectivity, we follow the discrete diffusion setting in (Vignac et al. 2022). The noise model q is represented by a sequence of transition matrices (Q^1, \dots, Q^T) . It acts on a one-hot encoding $x \in \mathbb{R}^d$ over d categories, where $[Q^t]_{i,j}$ indicates the probability of transferring the category i to j at

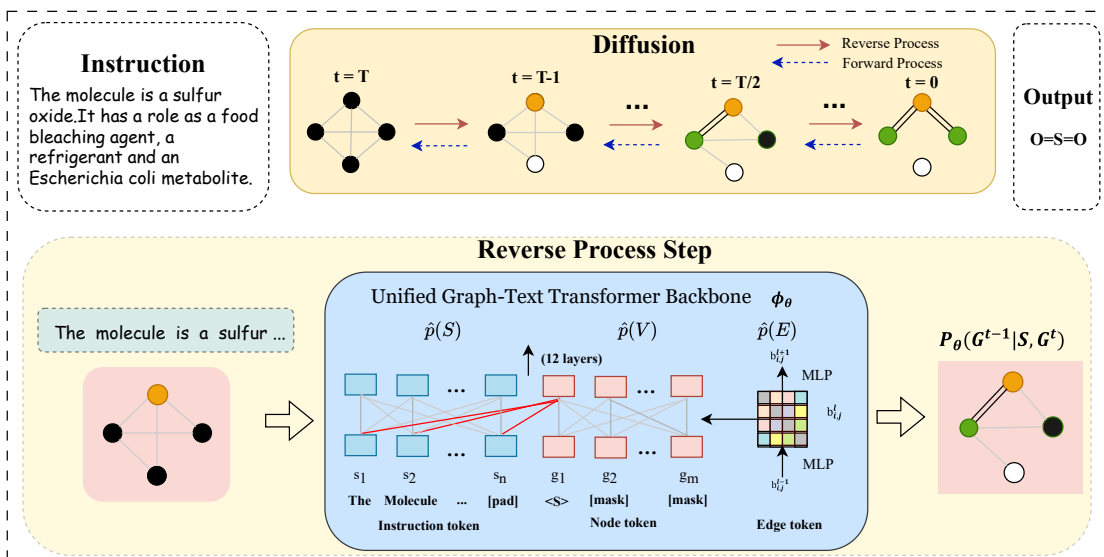


Figure 2: Overview of the UTGDiff framework. It incorporates attention bias into the vanilla transformer, forming a unified text-graph transformer that serves as a denoising network for discrete graph diffusion to generate molecular graphs from instructions. Noise decays some nodes and edges into [MASK] during training (forward process), with the reverse process aiming to recover original graphs as the training objective. Sampling starts with a masked graph and iterates T times to reduce noise.

time step t . We independently diffuse each one-hot category-based attribution in nodes V and edges E using separate matrices Q_V^t and Q_E^t . The forward process is:

$$q(G^t | G^{t-1}) = (V^{t-1} Q_V^t, E^{t-1} Q_E^t) \quad (2)$$

It can also be expressed as:

$$q(G^t | G^0) = (V \bar{Q}_V^t, E \bar{Q}_E^t) \quad (3)$$

$$\bar{Q}_V^t = Q_V^1 \dots Q_V^t, \quad \bar{Q}_E^t = Q_E^1 \dots Q_E^t$$

Specifically, we employ absorbing discrete diffusion (Austin et al. 2021), where each element v_i^t (and $e_{i,j}^t$) independently decays into an absorbing state based on the noise schedule probabilities. The absorbing state is defined as a [MASK] token, shared by text and graph tokens. Following the noise schedule $\beta(t) = (T - t + 1)^{-1}$, the corresponding transition matrix Q^t is formally expressed as follows, applying to both nodes and edges simultaneously, where z is the index for [MASK] token:

$$[Q^t]_{i,j} = \begin{cases} 1 & \text{if } i = j = z \\ 1 - \beta(t) & \text{if } i = j \neq z \\ \beta(t) & \text{if } j = z, i \neq z \end{cases} \quad (4)$$

Reverse Process and Denoising Network

Overview The reverse process relies on a denoising neural network ϕ_θ parameterized by θ . This network is trained to invert the forward process by predicting G^{t-1} from G^t using the text instruction S , formally represented as:

$$p_\theta(G^{0:T-1} | G^T, S) = \prod_{t=1}^T p_\theta(G^{t-1} | G^t, S). \quad (5)$$

As the formula indicates, the denoising network must simultaneously encode the textual instruction and graph to generate the probability distributions of nodes and edges at next time step. To ensure sufficient comprehension of instructions, we retain the transformer model and propose the *Unified Text-Graph Transformer* as our denoising network.

Tokenizer To adapt the vanilla transformer for processing graph data, we first address the representation of graph nodes by treating them as new tokens. The initial embeddings are denoted as $h^0 = \text{Emb}(S + V) = [h_1, \dots, h_n, h_{n+1}, \dots, h_{n+m}] \in \mathbb{R}^{(n+m) \times d_h}$, corresponding to m graph nodes and n text tokens, where h_1, \dots, h_n are encodings derived from the token list $S = [s_1, \dots, s_n]$ and h_{n+1}, \dots, h_{n+m} are encodings based on the categorical list of atoms in the molecule (e.g., [[S],[O],[O]] for sulfur oxide). Our model treats each graph category as a novel token to prevent interference from irrelevant tokens, thereby avoiding misrepresentations such as interpreting cobalt as a combination of carbon and oxygen.

Attention Bias Next, we address the representation of edges. In the attention layer, which includes parameters for values, keys, and outputs, i.e., $W_V, W_Q, W_K \in \mathbb{R}^{d_h \times d_k}$, $W_O \in \mathbb{R}^{d_k \times d_h}$, we introduce an additional bias term to incorporate edge information. The attention score between the i -th and j -th graph tokens is now formalized as:

$$\hat{A}_{i,j}^l = \frac{1}{\sqrt{d_k}} (h_i^l W_Q) (h_j^l W_K)' + b_{i,j}^l, \quad (6)$$

$$A^l = \text{softmax}(\hat{A}^l), \quad \text{Attn}(H) = A^l H^l W_V W_O$$

Here, $b_{i,j}$ represents the bias added to the graph tokens to

incorporate structural information (Ying et al. 2021; Chormanski et al. 2022; Park et al. 2022; Zhao et al. 2023). The most fundamental requirement for encoding graph data is the ability to distinguish whether two nodes in the graph are neighbors, which corresponds to the expressive power of a single-layer GNN (Xu et al. 2018). In addition, edge attribution must maintain symmetry for structural interpretability. Representing the initial embedding from the edge category as $b_{i,j}^0$, we therefore define the attention bias as follows:

$$b_{i,j}^l = \begin{cases} b_{i,j}^0, & \text{if } l = 0 \\ A_{i,j}^{l-1}, & \text{otherwise} \end{cases} \quad (7)$$

In addition to fulfilling the structural requirements outlined above and theoretically discussed in Appendix B, a vital advantage is that our model requires minimal modifications to existing language models, enabling them to process graph and text data simultaneously without additional graph neural network and benefiting from initial pre-trained weights. Moreover, our model enhances the integration of text and graph data, as the layer-level interactions between modalities facilitate a better alignment, allowing text information to be incorporated into graph data at multiple scales.

Output After obtaining the final hidden states h^L for tokens and b^L for edges through stacked attention layers, we map these hidden states back to the vocabulary space to determine the probability of each category for diffusion. We employ two separate masked language model heads for nodes and edges at the end of the transformer to decode these hidden states to the distribution of a clean graph.

Ultimately, we obtain the nodes logits $\log p_\theta(v_i | G^t, S)$ and edges logits $\log p_\theta(e_{i,j} | G^t, S)$ for a clean graph as output. Assembling these logits into matrices as $\hat{p}(V) \in \mathbb{R}^{m \times a}$, $\hat{p}(E) \in \mathbb{R}^{m \times m \times b}$, we summarize our unified text-graph denoising network as:

$$\phi_\theta(G^t, S) = \hat{p}(G) = [\hat{p}(V), \hat{p}(E)] \quad (8)$$

Sampling There remains a gap between the distribution of the clean graph and the required next-step distribution as formula (5). This gap is fixed through the x_0 -parameterization, which adds noise back to the clean graph prediction, represented as $p_\theta(G^{t-1} | G^t, S) = q(G^{t-1} | G^t, \phi_\theta(G^t, S))$, yielding a distribution from which G^{t-1} is sampled:

$$\begin{aligned} p_\theta(v_i^{t-1} | G^t, S) &= \sum_{v \in \mathcal{V}} q(v_i^{t-1} | v_i = v, v_i^t) \hat{p}_i(v) \\ p_\theta(e_{i,j}^{t-1} | G^t, S) &= \sum_{e \in \mathcal{E}} q(e_{i,j}^{t-1} | e_{i,j} = e, e_{i,j}^t) \hat{p}_{i,j}(e) \end{aligned} \quad (9)$$

Now sampling can be performed as Algorithm 2. It begins with graph G^T , where each node and edge is masked. At each step t , it calculates the distribution and samples the graph at step $t-1$, gradually reducing the noise and eventually resulting in a clean graph G^0 . Our model can implicitly sample the molecular length through the empty token, which is crucial as target molecule may be unique for instructions.

Training Objective

Since the denoising model takes a noisy graph G^t as input and aims to predict the clean graph G^0 , we optimize the cross-entropy loss (represented as CE) for each node and edge between the predicted probabilities $\hat{p}(G)$ and the clean graph G during training. The diffusion loss is defined as:

$$\begin{aligned} \text{loss} &= l(\hat{p}(V), V) + l(\hat{p}(E), E) \\ &= \sum_{1 \leq i \leq m} \text{CE}(v_i, \hat{p}_i(V)) + \sum_{1 \leq i, j \leq m} \text{CE}(e_{i,j}, \hat{p}_{i,j}(E)) \end{aligned} \quad (10)$$

In addition, as previously discussed, maintaining balanced training across different modalities is crucial to prevent the model from diminishing its text comprehension ability after extensive training, as the tokens of the graph and text are non-overlapping. To address this issue, we incorporate a textual loss component to preserve the model’s text comprehension capability, which is defined as the cross-entropy loss for each token between the predicted logits $\hat{p}(S)$ and the ground-truth token in the instruction. Through the denoising model, the logits can be directly obtained alongside $\hat{p}(V)$ following a masked language model head, expressed as $\phi_\theta(G^t, S) = [\hat{p}(S), \hat{p}(V), \hat{p}(E)]$. The final loss is thus represented as:

$$\text{loss} = l(\hat{p}(V), V) + l(\hat{p}(E), E) + l(\hat{p}(S), S) \quad (11)$$

See Algorithm 1 for the complete training procedure.

Algorithm 1: Training Algorithm

Input: A graph $G = (V, E)$ with description S

- 1: **repeat**
- 2: Sample $t \sim U(1, \dots, T)$
- 3: Sample $G^t \sim V\bar{Q}_V^t \times E\bar{Q}_E^t$
- 4: $\hat{p}(S), \hat{p}(V), \hat{p}(E) = \phi_\theta(G^t, S)$
- 5: $\text{loss} = l_{CE}(\hat{p}(E), E) + l_{CE}(\hat{p}(V), V) + l_{CE}(\hat{p}(S), S)$
- 6: optimizer.step(loss)
- 7: **until** converged

Algorithm 2: Sampling Algorithm

- 1: G^T with all masked nodes and edges
- 2: **for** $t = T$ to 1 **do**
- 3: $\hat{p}(V), \hat{p}(E) = \phi_\theta(G^t, S)$
- 4: $p_\theta(v_i^{t-1} | G^t, S) = \sum_v q(v_i^{t-1} | v_i = v, v_i^t) \hat{p}_i(v)$
- 5: $p_\theta(e_{i,j}^{t-1} | G^t, S) = \sum_e q(e_{i,j}^{t-1} | e_{i,j} = e, e_{i,j}^t) \hat{p}_{i,j}(e)$
- 6: $G^{t-1} \sim \prod_i p_\theta(v_i^{t-1} | G^t, S) \prod_{i,j} p_\theta(e_{i,j}^{t-1} | G^t, S)$
- 7: **end for**
- 8: **return** G^0

Pretraining Method

Recent studies have demonstrated that BERT can be viewed as a one-step [MASK] absorbing diffusion model (Devlin et al. 2019; Austin et al. 2021), since one-step noising replaces some tokens with [MASK] and denoising performs

Type	Model	#params	MACCS FTS \uparrow	RDKit FTS \uparrow	Morgan FTS \uparrow	FCD \downarrow	Exact \uparrow	Valid \uparrow
Specialist Auto-regressive (w.o. pretrain)	T5-small	77M	0.704	0.578	0.525	2.89	0.064	0.608
	T5-base	248M	0.731	0.605	0.545	2.48	0.069	0.660
	T5-large	783M	0.823	0.731	0.670	1.22	0.279	0.902
	BioT5-base (reproduce)	252M	0.821	0.708	0.633	1.67	0.071	1.000
Specialist Auto-regressive (pretrain)	MolT5-small	77M	0.703	0.568	0.517	2.49	0.079	0.721
	MolT5-base	248M	0.721	0.588	0.529	2.18	0.081	0.772
	MolT5-large	783M	0.834	0.746	0.684	1.20	0.311	0.905
	MolXPT	350M	0.859	0.757	0.667	0.45	0.215	0.983
	BioT5-base (reproduce)	252M	0.843	0.745	0.676	1.41	0.097	1.000
Text diffusion	tgm-dlm	125M	0.854	0.739	0.688	0.77	0.242	0.871
	tgm-dlm w/o corr	125M	0.874	0.771	0.722	0.89	0.242	0.789
LLM	chatgpt3.5 (0-shot)	7B	0.703	0.568	0.517	2.49	0.079	0.721
	Chatgpt3.5 (10-shot)	7B	0.847	0.708	0.624	0.57	0.139	0.887
Graph-based	Momu-S	113M	0.244	0.103	0.047	22.21	0.000	1.000
	UTGDiff (w.o. pretrain)	125M	0.867	0.763	0.695	0.92	0.227	0.856
	UTGDiff (pretrain)	125M	0.885	0.795	0.724	0.86	0.374	0.893

Table 1: Results of the instruction-based molecule generation on ChEBI-20 dataset for both with/without pretraining setting.

Model	names
molT5	C4, ZINC
BioT5	C4, Pubmed, ZINC (w./w.o. IUPAC), pubchem324K, bioRxiv, NER Wrapped biotext
UTGDiff	Pubmed, ZINC, pubchem324K

Table 2: Review of pretraining datasets. Some data listed in BioT5 is unavailable, and we reproduce it with our dataset.

masked prediction. This shared training objective allows for the effective initialization from pre-trained language models (He et al. 2022). Therefore, to preserve language comprehension, we utilize the pre-trained RoBERTa model (Liu et al. 2019) for initialization.

However, the introduction of novel graph tokens during tokenization renders the direct loading of pre-trained BERT/RoBERTa parameters insufficient for mask prediction on graph tokens. Consequently, our pretraining methods are designed to equip the model with mask prediction capabilities for graph data while retaining its functionality for text data. We collect paired or single-modal data in both text and molecular graph modalities, mask all tokens and edge indices with a 15% probability, and pretrain the model using the masked language prediction method. The effectiveness of this pretraining approach for graph data has been validated by previous studies on graph pretraining (Hu et al. 2020; Hou et al. 2022).

Experiment

Dataset

Pretraining Dataset We collect several open-source datasets for pretraining. For the molecule-text pair data, we select the PubChem-324K dataset (Liu et al. 2023c), which contains approximately 320,000 molecule-text pairs from PubChem. For the single-modal data, we utilize the molecular graph dataset ZINC20 (Irwin et al. 2020) and biomed-

model	1-64	65-96	97-128	129-160	> 160
BioT5 (reproduce)	0.810	0.866	0.859	0.817	0.788
UTGDiff	0.860	0.903	0.901	0.853	0.821

Table 3: Analysis for scalability on instruction length.

ical text data from PubMed abstracts (White 2020), totaling nearly 100 million entries. Due to computational budget constraints, we are unable to scale up the training size and batch size of the pretraining corpus to the extent achieved by BioT5 (Pei et al. 2023), which utilizes non-open-source pretraining data.

Generation Dataset For molecule generation tasks, we utilize the ChEBI-20 dataset (Edwards, Zhai, and Ji 2021) for finetuning and evaluation, which consists of 33,010 entries, with 10% allocated for validation and 10% for testing. We adhere to the original data split settings.

Editing Dataset For molecule editing, we select the retrosynthesis and forward reaction prediction tasks from Mol-Instructions (Fang et al. 2023). The retrosynthesis task begins with a target compound and identifies potential precursor molecules as outputs. The forward reaction prediction task involves forecasting likely products as output molecular graphs, given specific reactants and reagents. Each of these two datasets contains approximately 120,000 reactant-product pairs for training and 1,000 pairs for testing, with each entry accompanied by an instruction.

Baselines

Several prior studies have explored sequence-based models for evaluation. For the ChEBI-20 dataset, the baseline models include (1) specialist auto-regressive models such as T5 (Raffel et al. 2020), MolT5 (Edwards et al. 2022) and BioT5 (Pei et al. 2023); (2) LLMs such as ChatGPT-3.5

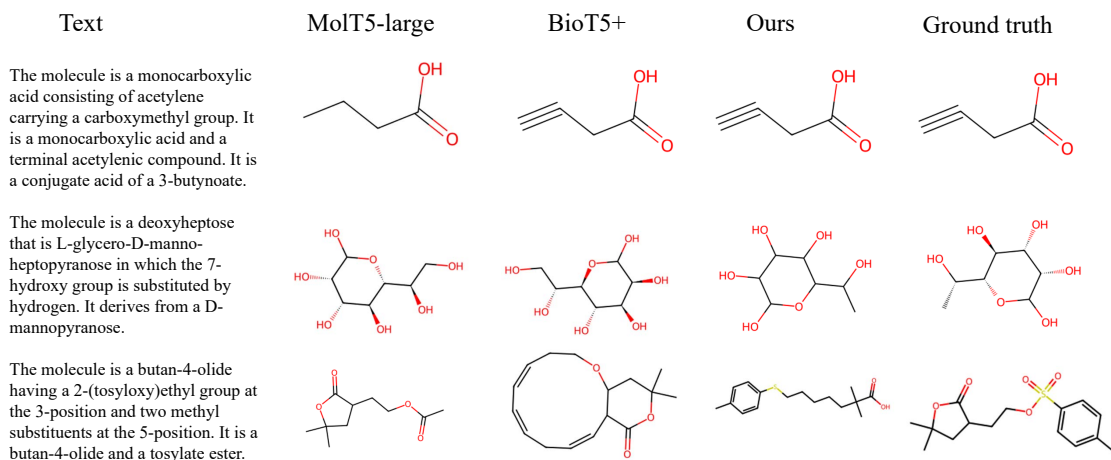


Figure 3: Some generation examples from our model and baseline models.

Type	Model	MACCS	RDk	Morgan	Exact	Valid
LLM	LLAMA	0.029	0.018	0.017	0.000	0.010
	GALACTICA	0.274	0.167	0.134	0.000	0.986
	Mol-Instructions	0.487	0.283	0.230	0.009	1.000
	Llama-7b* (LoRA)	0.294	0.136	0.106	0.000	1.000
	InstructMol-G	0.523	0.422	0.285	0.114	1.000
	InstructMol-GS	0.852	0.753	0.714	0.407	1.000
T5	TEXT+CHEM T5	0.765	0.685	0.585	0.141	0.698
	BioT5+ (reproduce)	0.904	0.843	0.810	0.480	1.000
UTGDiff		0.904	0.847	0.817	0.541	0.945

Table 4: Mol-Instruction Retrosynthesis results.

for zero-shot and 10-shot; and (3) text diffusion model tgm-dlm (Gong et al. 2024). For the editing datasets, the baseline models include (1) specialist auto-regressive models such as BioT5 (Pei et al. 2024) and TEXT+CHEM T5 (Christofidellis et al. 2023); (2) LLM such as InstructMol (Cao et al. 2023) and other models. Since BioT5’s pretraining data is not open-sourced, we reproduce their experiments training on our pretraining datasets using reported hyperparameters, rather than referencing their reported performance.

These baselines help us highlight the deficiencies of sequence-based models and clarify our improvements. Additionally, to assess the effectiveness of our diffusion method, we finetuned MoMu-S (Su et al. 2022) on the CHEBI-20 dataset for instruction-based generation. Due to the lack of capability to interpret language in the graph-only structure-aware network, there’re few baselines related to graph diffusion and it’s challenging to directly adapt them into these tasks. Therefore, we don’t consider them as baselines, but further discuss these methods in Ablation Study.

Instruction-Based Molecule Generation

Results Our results are shown in Table 1. The evaluation metrics are chosen based on previous studies, including a validity metric and five graph-level similarity metrics, with the exception of text-level similarity metrics such as BLEU.

Type	Model	MACCS	RDk	Morgan	Exact	Valid
LLM	LLAMA	0.002	0.001	0.001	0.000	0.010
	GALACTICA	0.127	0.036	0.051	0.000	0.995
	Mol-Instructions	0.509	0.313	0.262	0.045	1.000
	Llama-7b* (LoRA)	0.649	0.499	0.407	0.012	1.000
	InstructMol-G	0.717	0.519	0.457	0.114	1.000
	InstructMol-GS	0.878	0.776	0.741	0.407	1.000
T5	TEXT+CHEM T5	0.789	0.705	0.652	0.141	0.698
	BioT5+ (reproduce)	0.954	0.907	0.890	0.684	1.000
UTGDiff		0.973	0.943	0.942	0.825	0.972

Table 5: Mol-Instruction forward reaction prediction results.

Here, we present the results of a single experiment. Detailed descriptions of these metrics, additional results and variance obtained from different seeds, and details for experiments such as hyperparams are available in the supplementary material C,D. Our experimental findings are as follows:

Our model outperforms all auto-regressive methods across almost all similarity metrics with the same level of pretraining corpus. UTGDiff exhibits substantial improvements in the Exact match score, with gains of at least 6% over the best auto-regressive baseline. Also, UTGDiff achieves the highest FTS score, surpassing baseline models by at least 2%. These results indicate the methodological advantages of diffusion paradigm, since it is better suited to capturing the complex structures inherent in molecules.

Compared to text diffusion models, UTGDiff also performs better in both similarity and validity metrics. Especially, UTGDiff exhibits a remarkable 15% improvement in the Exact match score. This indicates that the superior performance of our model is not solely attributable to the diffusion paradigm. Instead, by incorporating graph-based representations, our model leverages explicit structural information in graph data processing, which is not attainable with text diffusion methods.

Our model is far better than the graph-based MoMu-S model. The low performance of MoMu-S may be attributed

model	steps	MACCS FTS \uparrow	Valid \uparrow	time(secs/sample) \downarrow
UTGDiff	1	0.838	0.515	0.861
	10	0.879	0.860	0.968
	100	0.885	0.893	1.929
	1000	0.881	0.901	11.388
BioT5	-	0.843	1.000	0.763

Table 6: Ablation study on diffusion framework. Steps = 1 is equal to without diffusion

Model	MACCS FTS \uparrow	FCD \downarrow	Valid \uparrow	Similarity \uparrow
w.o. unifying	0.583	28.47	0.753	-
3M-Diffusion	-	-	-	0.871
UTGDiff	0.867	0.923	0.856	0.957

Table 7: Ablation study on unifying denoising network.

to the limitations of MoFlow, as it struggles to follow complex instructions and generate long molecules, showing the importance of unified diffusion.

Our model has fewer parameters than other models with comparable performance. Our model has only 125M parameter size, smaller than other T5 models and LLMs.

Our model performs marginally worse than the reported results of BioT5+ and the recently finetuned LLM (Li et al. 2024). This can be attributed to the larger pretraining corpora they used as discussed in the ablation study. Also, our model shows minor shortcomings in validity metrics due to inevitable valence-induced invalidity. The low value in FCD can be attributed to misleading influences from other generated molecules, as discussed in supplementary material A.

Case Study We present several generated examples in Figure 3. The model successfully generates accurate results comparable to baseline models (Example 1). In some instances, it produces the correct solution when other models fail (Example 2). Also, it can effectively capture essential prompt words like "tosylate" and generate the required sulfur atom, demonstrating its capability to produce contextually appropriate outputs (Example 3).

Scalability on Instruction We also present an experiment assessing performance with varying complexities of instructions. We report the MACCS results for varying lengths of instructions and compare them with BioT5. The results indicate that our diffusion model achieves better outcomes across all intervals, demonstrating enhanced scalability when handling more complex instructions.

Instruction-Based Molecule Editing

We also conducted experiments on molecule editing tasks to demonstrate the model’s generalization capabilities across diverse tasks. Transferring from molecular generation to editing requires an additional source molecular graph as input, which is incorporated into the instruction input in graph format. The results are presented in Table 4 and Table 5.

Our model outperforms baseline models in all fingerprint and exact match metrics, with gains of at least 2%

Model	MACCS \uparrow	FCD \downarrow	Valid \uparrow	Train loss \downarrow	Entry
from scratch	0.867	0.923	0.856	1.58e-2	0
Pair-only	0.870	0.892	0.879	1.99e-3	300K
All	0.885	0.866	0.893	7.69e-4	100M

Table 8: Ablation study on pretrain data.

in forward reaction prediction tasks. These results underscore the methodological advantages of our model over previous string-based auto-regressive models. When compared to InstructMol-G and InstructMol-GS, our model exhibits a remarkable doubling of the exact match score in forward reaction prediction, with at least a 5% improvement in all metrics across both tasks. These results highlight the significance of the diffusion generation method for these tasks, as InstructMol-G incorporates a 2D molecular graph encoder while retaining a sequence-based decoder approach.

Ablation Study

In our ablation study, we validate our model focusing on the impact of pretraining and model design. All ablation experiments were performed using the CHEBI-20 dataset.

Model Design Our investigation of model design focuses on two key components to highlight the importance of novel modules: (a) Ablation of the diffusion module. Using the x_0 -parameterization, we can perform inference with flexible step size during the reverse process, while the one-step logits represent a scenario without diffusion. The effectiveness of the diffusion module is demonstrated in Table 6. (b) Ablation of the unified denoising network. This experiment involves the independent use of the graph diffusion network and text encoder, guided by a similarity gradient (Liu et al. 2023b), without the unification of the network. Additionally, we draw from the recent 3M-Diffusion model (Zhu, Xiao, and Honavar 2024), a text-guided graph diffusion method that employs separate encoders, and evaluate our generation results using their Similarity metrics. The results, shown in Table 7, indicate the effectiveness of the unified network.

Pretraining We conducted another ablation experiment to assess the impact of pretraining scale. The comparison, detailed in Table 8, highlights the critical roles of both single-modal and paired pretraining datasets and demonstrates the importance of scale, particularly concerning the validity.

Conclusions and Limitations

In this paper, we propose UTGDiff, an instruction-based framework that unifies graph and text data within a single transformer through attention bias, leveraging for the denoising generation of graph data. Our model is evaluated on tasks involving instruction-based molecule generation and editing, showing superior performance while requiring fewer parameters with the same level of pretraining corpus.

Several limitations constrain this research. A critical constraint is our inability to scale the pretraining corpus to a larger size, a factor that significantly benefits models like

BioT5 and may have limited our model’s ability to generalize across different molecular structures. Additionally, further experiments on more advanced discrete diffusion frameworks should be explored.

References

- Achiam, J.; Adler, S.; Agarwal, S.; Ahmad, L.; Akkaya, I.; Aleman, F. L.; Almeida, D.; Altschmidt, J.; Altman, S.; Anadkat, S.; et al. 2023. Gpt-4 technical report. *arXiv preprint arXiv:2303.08774*.
- AI4Science, M. R.; and Quantum, M. A. 2023. The impact of large language models on scientific discovery: a preliminary study using gpt-4. *arXiv preprint arXiv:2311.07361*.
- Arús-Pous, J.; Johansson, S. V.; Prykhodko, O.; Bjerrum, E. J.; Tyrchan, C.; Reymond, J.-L.; Chen, H.; and Engkvist, O. 2019. Randomized SMILES strings improve the quality of molecular generative models. *Journal of cheminformatics*, 11: 1–13.
- Askr, H.; Elgeldawi, E.; Aboul Ella, H.; Elshaier, Y. A.; Gomaa, M. M.; and Hassaniien, A. E. 2023. Deep learning in drug discovery: an integrative review and future challenges. *Artificial Intelligence Review*, 56(7): 5975–6037.
- Austin, J.; Johnson, D. D.; Ho, J.; Tarlow, D.; and Van Den Berg, R. 2021. Structured denoising diffusion models in discrete state-spaces. *Advances in Neural Information Processing Systems*, 34: 17981–17993.
- Bagal, V.; Aggarwal, R.; Vinod, P.; and Priyakumar, U. D. 2021. MolGPT: molecular generation using a transformer-decoder model. *Journal of Chemical Information and Modeling*, 62(9): 2064–2076.
- Cao, H.; Liu, Z.; Lu, X.; Yao, Y.; and Li, Y. 2023. Instructmol: Multi-modal integration for building a versatile and reliable molecular assistant in drug discovery. *arXiv preprint arXiv:2311.16208*.
- Choromanski, K.; Lin, H.; Chen, H.; Zhang, T.; Sehanobish, A.; Likhoshesterov, V.; Parker-Holder, J.; Sarlos, T.; Weller, A.; and Weingarten, T. 2022. From block-Toeplitz matrices to differential equations on graphs: towards a general theory for scalable masked Transformers. In *International Conference on Machine Learning*, 3962–3983. PMLR.
- Christofidellis, D.; Giannone, G.; Born, J.; Winther, O.; Laino, T.; and Manica, M. 2023. Unifying molecular and textual representations via multi-task language modelling. In *International Conference on Machine Learning*, 6140–6157. PMLR.
- Dai, H.; Tian, Y.; Dai, B.; Skiena, S.; and Song, L. 2018. Syntax-directed variational autoencoder for structured data. *arXiv preprint arXiv:1802.08786*.
- De Cao, N.; and Kipf, T. 2018. MolGAN: An implicit generative model for small molecular graphs. *arXiv preprint arXiv:1805.11973*.
- Devlin, J.; Chang, M.-W.; Lee, K.; and Toutanova, K. 2019. Bert: Pre-training of deep bidirectional transformers for language understanding. *Proceedings of the 2019 Conference of the North American Chapter of the Association for Computational Linguistics: Human Language Technologies, Volume 1 (Long and Short Papers)*.
- Dickson, M.; and Gagnon, J. P. 2009. The cost of new drug discovery and development. *Discovery medicine*, 4(22): 172–179.
- Druchok, M.; Yarish, D.; Gurbych, O.; and Maksymenko, M. 2021. Toward efficient generation, correction, and properties control of unique drug-like structures. *Journal of Computational Chemistry*, 42(11): 746–760.
- Durant, J. L.; Leland, B. A.; Henry, D. R.; and Nourse, J. G. 2002. Reoptimization of MDL keys for use in drug discovery. *Journal of chemical information and computer sciences*, 42(6): 1273–1280.
- Edwards, C.; Lai, T.; Ros, K.; Honke, G.; Cho, K.; and Ji, H. 2022. Translation between molecules and natural language. *arXiv preprint arXiv:2204.11817*.
- Edwards, C.; Zhai, C.; and Ji, H. 2021. Text2mol: Cross-modal molecule retrieval with natural language queries. In *Proceedings of the 2021 Conference on Empirical Methods in Natural Language Processing*, 595–607.
- Fang, Y.; Liang, X.; Zhang, N.; Liu, K.; Huang, R.; Chen, Z.; Fan, X.; and Chen, H. 2023. Mol-instructions: A large-scale biomolecular instruction dataset for large language models. *arXiv preprint arXiv:2306.08018*.
- Gómez-Bombarelli, R.; Wei, J. N.; Duvenaud, D.; Hernández-Lobato, J. M.; Sánchez-Lengeling, B.; Sheberla, D.; Aguilera-Iparraguirre, J.; Hirzel, T. D.; Adams, R. P.; and Aspuru-Guzik, A. 2018. Automatic chemical design using a data-driven continuous representation of molecules. *ACS central science*, 4(2): 268–276.
- Gong, H.; Liu, Q.; Wu, S.; and Wang, L. 2024. Text-Guided Molecule Generation with Diffusion Language Model. *Proceedings of the AAAI Conference on Artificial Intelligence*, 38(1): 109–117.
- Grisoni, F.; Moret, M.; Lingwood, R.; and Schneider, G. 2020. Bidirectional molecule generation with recurrent neural networks. *Journal of chemical information and modeling*, 60(3): 1175–1183.
- Hartenfeller, M.; and Schneider, G. 2011. De novo drug design. *Chemoinformatics and computational chemical biology*, 299–323.
- He, Z.; Sun, T.; Wang, K.; Huang, X.; and Qiu, X. 2022. Diffusionbert: Improving generative masked language models with diffusion models. *arXiv preprint arXiv:2211.15029*.
- Hou, Z.; Liu, X.; Cen, Y.; Dong, Y.; Yang, H.; Wang, C.; and Tang, J. 2022. Graphmae: Self-supervised masked graph autoencoders. In *Proceedings of the 28th ACM SIGKDD Conference on Knowledge Discovery and Data Mining*, 594–604.
- Hu, Z.; Dong, Y.; Wang, K.; Chang, K.-W.; and Sun, Y. 2020. Gpt-gnn: Generative pre-training of graph neural networks. In *Proceedings of the 26th ACM SIGKDD international conference on knowledge discovery & data mining*, 1857–1867.
- Huang, H.; Sun, L.; Du, B.; and Lv, W. 2023. Conditional diffusion based on discrete graph structures for molecular graph generation. In *Proceedings of the AAAI Conference on Artificial Intelligence*, volume 37, 4302–4311.

- Hughes, J. P.; Rees, S.; Kalindjian, S. B.; and Philpott, K. L. 2011. Principles of early drug discovery. *British journal of pharmacology*, 162(6): 1239–1249.
- Irwin, J. J.; Tang, K. G.; Young, J.; Dandarchuluun, C.; Wong, B. R.; Khurelbaatar, M.; Moroz, Y. S.; Mayfield, J.; and Sayle, R. A. 2020. ZINC20—a free ultralarge-scale chemical database for ligand discovery. *Journal of chemical information and modeling*, 60(12): 6065–6073.
- Jiang, J.; Zhang, R.; Zhao, Z.; Ma, J.; Liu, Y.; Yuan, Y.; and Niu, B. 2022. MultiGran-SMILES: multi-granularity SMILES learning for molecular property prediction. *Bioinformatics*, 38(19): 4573–4580.
- Jin, W.; Barzilay, R.; and Jaakkola, T. 2018. Junction tree variational autoencoder for molecular graph generation. In *International conference on machine learning*, 2323–2332. PMLR.
- Jo, J.; Lee, S.; and Hwang, S. J. 2022. Score-based generative modeling of graphs via the system of stochastic differential equations. In *International Conference on Machine Learning*, 10362–10383. PMLR.
- Khanna, I. 2012. Drug discovery in pharmaceutical industry: productivity challenges and trends. *Drug discovery today*, 17(19-20): 1088–1102.
- Kong, L.; Cui, J.; Sun, H.; Zhuang, Y.; Prakash, B. A.; and Zhang, C. 2023. Autoregressive diffusion model for graph generation. In *International conference on machine learning*, 17391–17408. PMLR.
- Krenn, M.; Häse, F.; Nigam, A.; Friederich, P.; and Aspuru-Guzik, A. 2020. Self-referencing embedded strings (SELFIES): A 100% robust molecular string representation. *Machine Learning: Science and Technology*, 1(4): 045024.
- Li, J.; Liu, W.; Ding, Z.; Fan, W.; Li, Y.; and Li, Q. 2024. Large Language Models are In-Context Molecule Learners. *arXiv preprint arXiv:2403.04197*.
- Li, J.; Liu, Y.; Fan, W.; Wei, X.-Y.; Liu, H.; Tang, J.; and Li, Q. 2023. Empowering molecule discovery for molecule-caption translation with large language models: A chatgpt perspective. *arXiv preprint arXiv:2306.06615*.
- Li, Y.; Zhang, L.; and Liu, Z. 2018. Multi-objective de novo drug design with conditional graph generative model. *Journal of cheminformatics*, 10: 1–24.
- Liang, Y.; Zhang, R.; Zhang, L.; and Xie, P. 2023. DrugChat: towards enabling ChatGPT-like capabilities on drug molecule graphs. *arXiv preprint arXiv:2309.03907*.
- Liu, P.; Ren, Y.; Tao, J.; and Ren, Z. 2024. Git-mol: A multi-modal large language model for molecular science with graph, image, and text. *Computers in Biology and Medicine*, 171: 108073.
- Liu, Q.; Allamanis, M.; Brockschmidt, M.; and Gaunt, A. 2018. Constrained graph variational autoencoders for molecule design. *Advances in neural information processing systems*, 31.
- Liu, S.; Nie, W.; Wang, C.; Lu, J.; Qiao, Z.; Liu, L.; Tang, J.; Xiao, C.; and Anandkumar, A. 2023a. Multi-modal molecule structure–text model for text-based retrieval and editing. *Nature Machine Intelligence*, 5(12): 1447–1457.
- Liu, X.; Park, D. H.; Azadi, S.; Zhang, G.; Chopikyan, A.; Hu, Y.; Shi, H.; Rohrbach, A.; and Darrell, T. 2023b. More control for free! image synthesis with semantic diffusion guidance. In *Proceedings of the IEEE/CVF Winter Conference on Applications of Computer Vision*, 289–299.
- Liu, Y.; Ott, M.; Goyal, N.; Du, J.; Joshi, M.; Chen, D.; Levy, O.; Lewis, M.; Zettlemoyer, L.; and Stoyanov, V. 2019. Roberta: A robustly optimized bert pretraining approach. *arXiv preprint arXiv:1907.11692*.
- Liu, Z.; Li, S.; Luo, Y.; Fei, H.; Cao, Y.; Kawaguchi, K.; Wang, X.; and Chua, T.-S. 2023c. Molca: Molecular graph-language modeling with cross-modal projector and unimodal adapter. *arXiv preprint arXiv:2310.12798*.
- Liu, Z.; Zhang, W.; Xia, Y.; Wu, L.; Xie, S.; Qin, T.; Zhang, M.; and Liu, T.-Y. 2023d. Molxpt: Wrapping molecules with text for generative pre-training. *arXiv preprint arXiv:2305.10688*.
- Ma, C.; and Zhang, X. 2021. GF-VAE: a flow-based variational autoencoder for molecule generation. In *Proceedings of the 30th ACM international conference on information & knowledge management*, 1181–1190.
- Miller, F. P.; Vandome, A. F.; and McBrewster, J. 2009. Levenshtein distance: Information theory, computer science, string (computer science), string metric, damerau? Levenshtein distance, spell checker, hamming distance.
- Nag, S.; Baidya, A. T.; Mandal, A.; Mathew, A. T.; Das, B.; Devi, B.; and Kumar, R. 2022. Deep learning tools for advancing drug discovery and development. *3 Biotech*, 12(5): 110.
- Niu, C.; Song, Y.; Song, J.; Zhao, S.; Grover, A.; and Ermon, S. 2020. Permutation invariant graph generation via score-based generative modeling. In *International Conference on Artificial Intelligence and Statistics*, 4474–4484. PMLR.
- O’Boyle, N.; and Dalke, A. 2018. DeepSMILES: an adaptation of SMILES for use in machine-learning of chemical structures.
- Papineni, K.; Roukos, S.; Ward, T.; and Zhu, W.-J. 2002. Bleu: a method for automatic evaluation of machine translation. In *Proceedings of the 40th annual meeting of the Association for Computational Linguistics*, 311–318.
- Park, W.; Chang, W.; Lee, D.; Kim, J.; and Hwang, S.-w. 2022. Grpe: Relative positional encoding for graph transformer. *arXiv preprint arXiv:2201.12787*.
- Pei, Q.; Wu, L.; Gao, K.; Liang, X.; Fang, Y.; Zhu, J.; Xie, S.; Qin, T.; and Yan, R. 2024. BioT5+: Towards Generalized Biological Understanding with IUPAC Integration and Multi-task Tuning. *arXiv preprint arXiv:2402.17810*.
- Pei, Q.; Zhang, W.; Zhu, J.; Wu, K.; Gao, K.; Wu, L.; Xia, Y.; and Yan, R. 2023. Biot5: Enriching cross-modal integration in biology with chemical knowledge and natural language associations. *arXiv preprint arXiv:2310.07276*.
- Preuer, K.; Renz, P.; Unterthiner, T.; Hochreiter, S.; and Klambauer, G. 2018. Fréchet ChemNet distance: a metric for generative models for molecules in drug discovery. *Journal of chemical information and modeling*, 58(9): 1736–1741.

- Raffel, C.; Shazeer, N.; Roberts, A.; Lee, K.; Narang, S.; Matena, M.; Zhou, Y.; Li, W.; and Liu, P. J. 2020. Exploring the limits of transfer learning with a unified text-to-text transformer. *Journal of machine learning research*, 21(140): 1–67.
- Rogers, D.; and Hahn, M. 2010. Extended-connectivity fingerprints. *Journal of chemical information and modeling*, 50(5): 742–754.
- Schneider, G.; and Fechner, U. 2005. Computer-based de novo design of drug-like molecules. *Nature Reviews Drug Discovery*, 4(8): 649–663.
- Schneider, N.; Sayle, R. A.; and Landrum, G. A. 2015. Get Your Atoms in Order - An Open-Source Implementation of a Novel and Robust Molecular Canonicalization Algorithm. *Journal of chemical information and modeling*, 55(10): 2111–2120.
- Schneuing, A.; Du, Y.; Harris, C.; Jamasb, A.; Igashov, I.; Du, W.; Blundell, T.; Lió, P.; Gomes, C.; Welling, M.; et al. 2022. Structure-based drug design with equivariant diffusion models. *arXiv preprint arXiv:2210.13695*.
- Simonovsky, M.; and Komodakis, N. 2018. Graphvae: Towards generation of small graphs using variational autoencoders. In *Artificial Neural Networks and Machine Learning–ICANN 2018: 27th International Conference on Artificial Neural Networks, Rhodes, Greece, October 4–7, 2018, Proceedings, Part I* 27, 412–422. Springer.
- Song, Y.; Zheng, S.; Niu, Z.; Fu, Z.-H.; Lu, Y.; and Yang, Y. 2020. Communicative Representation Learning on Attributed Molecular Graphs. In *IJCAI*, volume 2020, 2831–2838.
- Su, B.; Du, D.; Yang, Z.; Zhou, Y.; Li, J.; Rao, A.; Sun, H.; Lu, Z.; and Wen, J.-R. 2022. A molecular multimodal foundation model associating molecule graphs with natural language. *arXiv preprint arXiv:2209.05481*.
- Vignac, C.; Krawczuk, I.; Siraudin, A.; Wang, B.; Cevher, V.; and Frossard, P. 2022. Digress: Discrete denoising diffusion for graph generation. *arXiv preprint arXiv:2209.14734*.
- Weininger, D. 1988. SMILES, a chemical language and information system. 1. Introduction to methodology and encoding rules. *Journal of chemical information and computer sciences*, 28(1): 31–36.
- White, J. 2020. PubMed 2.0. *Medical reference services quarterly*, 39(4): 382–387.
- Wu, T.; Tang, Y.; Sun, Q.; and Xiong, L. 2023. Molecular joint representation learning via multi-modal information of smiles and graphs. *IEEE/ACM Transactions on Computational Biology and Bioinformatics*, 20(5): 3044–3055.
- Xu, K.; Hu, W.; Leskovec, J.; and Jegelka, S. 2018. How powerful are graph neural networks? *arXiv preprint arXiv:1810.00826*.
- Xu, M.; Yu, L.; Song, Y.; Shi, C.; Ermon, S.; and Tang, J. 2022. Geodiff: A geometric diffusion model for molecular conformation generation. *arXiv preprint arXiv:2203.02923*.
- Ye, G.; Cai, X.; Lai, H.; Wang, X.; Huang, J.; Wang, L.; Liu, W.; and Zeng, X. 2023. Drugassist: A large language model for molecule optimization. *arXiv preprint arXiv:2401.10334*.
- Ying, C.; Cai, T.; Luo, S.; Zheng, S.; Ke, G.; He, D.; Shen, Y.; and Liu, T.-Y. 2021. Do transformers really perform badly for graph representation? *Advances in neural information processing systems*, 34: 28877–28888.
- You, J.; Ying, R.; Ren, X.; Hamilton, W.; and Leskovec, J. 2018. Graphrnn: Generating realistic graphs with deep autoregressive models. In *International conference on machine learning*, 5708–5717. PMLR.
- Zang, C.; and Wang, F. 2020. Moflow: an invertible flow model for generating molecular graphs. In *Proceedings of the 26th ACM SIGKDD international conference on knowledge discovery & data mining*, 617–626.
- Zhao, H.; Liu, S.; Chang, M.; Xu, H.; Fu, J.; Deng, Z.; Kong, L.; and Liu, Q. 2024. Gimlet: A unified graph-text model for instruction-based molecule zero-shot learning. *Advances in Neural Information Processing Systems*, 36.
- Zhao, H.; Ma, S.; Zhang, D.; Deng, Z.-H.; and Wei, F. 2023. Are more layers beneficial to graph transformers? *arXiv preprint arXiv:2303.00579*.
- Zhu, H.; Xiao, T.; and Honavar, V. G. 2024. 3M-Diffusion: Latent Multi-Modal Diffusion for Text-Guided Generation of Molecular Graphs. *arXiv preprint arXiv:2403.07179*.

Supplementary Material

A. Analysis of FCD

FCD is a metric originally used to measure the distance between two sets of distributions. Previous works employed this metric to compare the distance between the ground-truth test sets and generation sets in instruction-based molecule generation tasks, rather than comparing the similarity one by one as other metrics do.

Since this metric compares the distance between molecule distributions, it can be misled by molecules generated from other instructions. For example, FCD is equivariant under reordering, meaning it cannot distinguish errors where generated molecules and instructions are exactly cross-matched. For instance, the instruction S_1 match the molecule ‘CCO’, and instruction S_2 match the molecule ‘[He]’. If we generate ‘CC’ with instruction S_1 and ‘[He]’ with instruction S_2 , there’s no doubt that $FCD(['CCO'], ['He'], ['CC'], ['He']) \neq 0$. However, If we generate ‘[He]’ with instruction S_1 and ‘CCO’ with instruction S_2 , which is a totally irrelevant results, we’ll got an unexpected result $FCD(['CCO'], ['He'], ['[He]', 'CCO']) = 0$.

To demonstrate the effectiveness of our model in FCD, we divided the test set into 10 subsets and calculated the average and variance FCD across them. This method can partially reduce interference between different instructions. We include tgm-dlm for comparison, as it has a lower FCD, while MolXPT is not open-sourced.

Using this processing method, our model achieved better FCD results, as shown in Table 9. The difference in magnitude between the two settings is an inherent property of FCD, which is related to the number of molecule sets.

B. Proof of required property

The edge attribution must maintain symmetry. This is conducted since the start of embedding is symmetrical as they have same categories. And therefore the edge attribution maintains symmetry in each layer.

Another required property for graph generation model is to ensure that the node’s attribution in the graph is equivariant to reorderings, meaning that the matrices under reordering can represent the same graph. This property requires no positional embedding in the denoising network. However, we empirically found the importance of positional embedding for better performance.

We attribute this result to the rich position information in the text description, as shown in figure 4. So, the model will lose its perception of this essential information without position embedding. This issue is more significant in diffusion models since the located step must be later than the decoding of the atom.

Therefore, to ensure equivariance on the inference step while retaining the utilization of position embedding, We adopt the following strategy: We use position embedding as before during training and make a random permutation of the position index in sequence during inference. It can be proven that the model is still equivariant during generation, although it is trained to fit a specific order of decoding atoms.

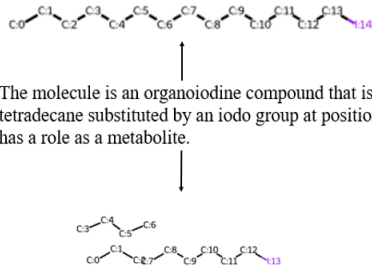


Figure 4: An example of generation results w/w.o position embedding. Adding position embedding can locate the position of the iodo group.

The theorem to be proven in this section can be written as follows:

Theorem 1 (Equivariancy for Graph Generation) *For any permutation π , the model will generate a graph with node feature V and adjacency matrix A with input position index i , satisfying $P_i(V, A) = P_{\pi^{-1}(i)}(\pi^T V, \pi^T A)$.*

The proof aims to show that: If the model’s network architecture is equivariant with input mapping permutation and the training loss is permutation invariant, the model will generate a distribution reordering with position index.

Lemma 1 *The loss in training is invariant under reordering: For given predict graph \hat{G} and ground truth graph G , given a permutation π , we have $l(\pi \cdot \hat{G}, \pi \cdot G) = l(\hat{G}, G)$*

Proof 1 *Since the defined loss function is the same for each node and edge, we have*

$$\begin{aligned} l(\pi \cdot \hat{G}, \pi \cdot G) &= \sum_i l_X(\pi \cdot \hat{X}_i, x_{\pi^{-1}(i)}) \\ &\quad + \sum_{i,j} l_E(\pi \cdot \hat{E}_{i,j}, e_{\pi^{-1}(i), \pi^{-1}(j)}) \\ &= \sum_i l_X(\hat{X}_i, x_i) + \sum_{i,j} l_E(\hat{E}_{i,j}, e_{i,j}) \\ &= l(\hat{G}, G) \end{aligned}$$

Lemma 2 *The architecture of the model is equivariant with the input embedding: For given predict graph \hat{G} and ground truth graph G , given a permutation π , we have $\phi_\theta(\pi \cdot G^t) = \pi \cdot \phi_\theta(G^t)$*

Proof 2 *Define $G_t = (X_t, E_t)$ as the noisy graph, $(\pi \cdot X_t, \pi \cdot E_t)$ as the permutation. Since the input is permutation equivariant, and we have:*

- The self attention architecture is permutation invariant
- The linear layers are permutation invariant.
- The Layer normalization is permutation equivariant.

Therefore, the model is a combination of permutation equivariant blocks.

Model	10 subset (new)	1 set (origin)
Tgm-dlm	3.38 ± 0.078	0.77
UTGDiff	3.25 ± 0.055	0.866

Table 9: FCD comparison

Proof 3 proof of theorem 1

For the input embedding after model permutation, we have $\pi^T X + \pi^T \text{emb}(i) = \pi^T (X + \text{emb}(i))$. Therefore, the assumption of input mapping permutation equivariant holds.

Following the proof in DiGress, with the lemma(Xu et al. 2022): if a distribution $p(G_T)$ is invariant to the action of a group G and the transition probabilities $p(G_{t-1}|G_t)$ are equivariant, then $p(G_0)$ is invariant to the action of G . We apply this result to the special case of permutations:

- The initial noise distribution is the mask distribution on each node and edge. It is therefore permutation invariant.
- The denoising neural networks is permutation equivariant.
- The transition probabilities function $p_\theta(G_{t-1}|G_t) = \sum_G q(G_{t-1}, G|G_t) \hat{p}_\theta(G)$ is equivariant to $\bar{p}_\theta(G)$ and G_T .

The conditions are therefore satisfied, and the model satisfies $P_i(V, A) = P_{\pi^T i}(\pi^T V, \pi^T A \pi)$.

C. Details for evaluation metrics

Since the model generates a matrix of nodes and edges, although ultimately a SMILES will be parsed based on the matrix, it is not directly generated, which can easily cause the problem of different strings for same graph. Therefore, although molecules can be represented by biological sequence structures, and previous models have also established evaluation indicators from the level of string similarity, this article does not involve these indicators in comparison, including NLP indicators such as BLEU(Papineni et al. 2002), Levenshtein(Miller, Vandome, and McBrewster 2009).

Therefore, we use a series of metrics related to the similarity of molecular graphs:

- Exact: Whether the two molecules are same.
- Valid: Whether the generated molecule satisfied the constraint for molecule, such as the valence rule.
- FTS: We employ three fingerprint metrics: MACCS FTS, RDK FTS, and Morgan FTS, where FTS stands for fingerprint Tanimoto similarity. MACCS (Durant et al. 2002), RDK(Schneider, Sayle, and Landrum 2015) and Morgan(Rogers and Hahn 2010). The fingerprints of two molecules are compared using Tanimoto similarity (also known as Jaccard index), and the average similarity over the evaluation dataset is reported. We use RDKit toolkit.
- FCD score (Fréchet chemnet distance)(Preuer et al. 2018): Measure molecular similarity based on a pre-trained "ChemNet" bioinformatics network. We use fcd 1.1 in python.

Model	MACCS ↑	RDk ↑	Morgan ↑	FCD ↓	Exact ↑	Valid ↑
baseline	0.867	0.763	0.695	0.923	0.227	0.856
acc_step = 4	0.838	0.719	0.629	1.651	0.149	0.792

Table 10: ablation of accumulation step (from-scratch)

param name	value
learning rate	5e-5
batch size	16
accumulation step	(1,4,16,64)
accumulation update epoch	(1,4,16,64)
top k	15
predict molecule length	128
seed	42
step size	20

Table 11: Hyperparam for CHEBI-20 datasets

D. Details for experiments

Here’re the hyperparam for three different tasks describe in article, and here’s some general information on hyperparam:

(1) The pretraining process spans nearly 300K steps and is executed on four NVIDIA 24GB GeForce RTX 3090 GPUs with batch size 32 per GPU, totally trained for near 1 week. The finetuning process spans nearly 800K steps and is executed on two NVIDIA 24GB GeForce RTX 3090 GPUs with batch size 16 per GPU, totally trained for near 3 days.

(2) During finetuning, we gradually increase the accumulation step for the tradeoff of training efficiency and convergence level. The effective of this method is shown in the ablation of accumulation step shown in Table 10. So, the initial accumulation step is 1, and it will be increase to 64 finally.

(3) When the model is used for generation, we additionally introduces top-k sampling to help improve the quality of generation: when a class is taken from the calculated probability for discrete generation, only the larger node class is taken.

(4) All the training and generation program is running under specific seed. We only generate onces, but experiments shows there’s no significant variance during sampling for different seeds. We show the 3 seed example in forward reaction prediction in Table 14

The specific data is listed in Table 11, 12, 13

Prompt Here we list the prompt for the three datasets: For CHEBI-20 dataset, We give its instruction form as : "[molecule description]" is the description of molecule." For the two editing dataset, since there’s task instruction in datasets, we don’t use any additional instructions. Here’s an example in Retrosynthesis dataset: "Please suggest potential reactants for the given product."; Here’s an example in forward reaction prediction dataset: "With the provided reactants and reagents, propose a potential product."

param name	value
learning rate	5e-5
batch size	16
accumulation step	(1,4,16,64)
epoch	1000
accumulation update epoch	(90,150,180)
top k	15
predict molecule length	108
seed	42
step size	10

Table 12: Hyperparam for Retrosynthesis datasets

param name	value
learning rate	5e-5
batch size	16
accumulation step	(1,4,16,64)
epoch	210
accumulation update epoch	(90,150,180)
top k	15
predict molecule length	96
seed	42
step size	10

Table 13: Hyperparam for forward reaction prediction datasets

Type	Model	MACCS	RDK	Morgan	Exact	Valid
seed 0		0.971	0.938	0.938	0.821	0.973
seed 1		0.974	0.940	0.938	0.825	0.968
seed 42		0.973	0.943	0.942	0.825	0.972

Table 14: 3 seeds for forward reaction prediction results

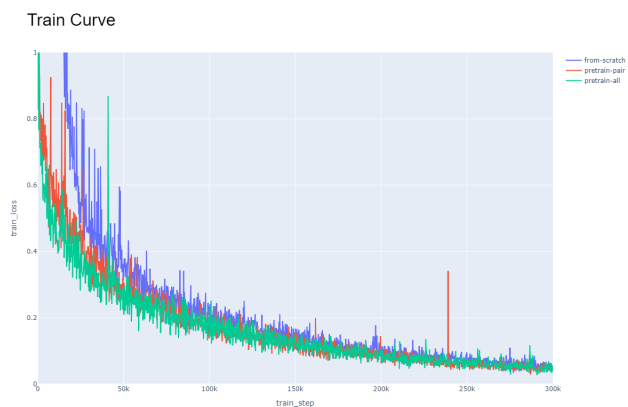


Figure 5: The training curve in first 300K steps. Pretraining also demonstrates lower initial loss and faster convergence compared to training models from scratch.

E. Source of datasets

All the datasets we used are open-sourced, can be found in github or huggingface:

huggingface: ZINC(zpn/zinc20); Pubmed; Pubchem

github: Mol-instruction, CHEBI-20